Kinetic Model for Metal-Organic Chemical Vapor Deposition of GaAs with Organometallic-Arsenic Precursors

Thomas R. Omstead† and Klavs F. Jensen*,‡

Department of Chemical Engineering and Materials Science, University of Minnesota, Minneapolis, Minnesota 55455

Received August 18, 1989

Models for the chemical kinetics of the growth of GaAs by using triethylgallium and trimethylgallium with trimethylarsene, triethylarsene, *tert*-butylarsine, and phenylarsine are described. Emphasis is placed on results obtained with a metal-organic chemical vapor deposition reactor equipped with a recording microbalance for in situ growth rate measurements. Rate data show that the growth with these precursors is dominated by adduct-related parasitic gas-phase reactions at high temperatures and by surface reactions at lower temperatures. A model is proposed for the competition between deposition reactions and the parasitic gas-phase reactions. The kinetic model works well for all combinations of precursors except for triethylgallium and trimethylarsene, where extensive gallium droplet formation is observed at low temperatures. The predicted rate constants reflect the trends expected from the chemical structure of the arsenic precursors and their tendency to form adduct compounds. In addition to the chemical investigations, the electrical properties of GaAs grown with triethylgallium and *tert*-butylarsine are examined by using the Hall effect. This source combination, which has not been used previously, gives promising results for the growth of GaAs.

Introduction

The use of arsine in metal-organic chemical vapor deposition (MOCVD) of GaAs has been demonstrated to give excellent electrical properties.[1] However, its use has a number of disadvantages primarily related to its toxicity and storage as a high-pressure gas.[2-4] Trimethylarsene (Me_3As),[5] triethylarsene (Et_3As),[6] diethylarsene (Et_2AsH),[7] *tert*-butylarsine (*t*-$BuAsH_2$),[8,9] and phenylarsine ($PhAsH_2$)[10] are alternative organometallic arsenic sources of arsine with the potential for growing good quality GaAs films at relatively low V/III ratios. Although considerable progress has been made toward this goal, electrical properties comparable with the best results obtained by using arsine have not yet been achieved.[11,12] However, organometallic precursors have been studied only for a brief time as compared to arsine. Therefore, it is difficult to distinguish if the inferior electrical properties achieved with them are the result of problems inherent in their use or if they are due to extrinsic impurities. Thus, when comparing the various organometallic precursors, it is necessary to focus on the fundamental chemistry associated with their use as well as on the best electrical and optical properties obtained.

Among the factors that determine the chemical behavior of an organometallic arsine derivative and its usefulness in MOCVD applications are the number of substituted organic ligands and their type. The number of alkyl ligands substituted in place of hydrogen appears to be particularly important.[2-4] Hydrogen directly attached to arsenic is believed to be responsible for removing adsorbed hydrocarbon species, such as methyl from Me_3Ga, from the surface before they decompose and lead to incorporation of carbon into the film. This is evidenced by Table I, which shows that the highest mobility reported for each arsenic compound decreases with increasing degree of alkyl substitution. The same arsenic-attached hydrogen atoms (Table I) are responsible for the extreme toxicity of arsine and its mono- or disubstituted derivatives. This is shown by the decrease in LC_{50} (ppm, 50% of animals dead after a 4-h exposure) with an increasing number of ligands.

Table I. Toxicity and Representative Mobility Data for Arsine and Organometallic Arsenic Compounds

source	alkyl substituted	mobility (77 K)	LC_{50}, ppm[4]
AsH_3	0	210 000[13]	5-50
t-$BuAsH_2$	1	85 000[14]	50-75
DEAs	2	64 600[9]	300
Et_3As	3	14 000[8]	500-1000
Me_3As	3	3 000[7]	20 000
$PhAsH_2$	(1)	38 000[12]	unknown

Table II. Radical-Hydrogen Bond Strengths and Decomposition Temperature

group	deg of alkyl substitution on α carbon	C-H bond strength, kcal/mol[17]	dec temp, °C
H		104.2	560 (AsH_3)[18]
methyl	0	104	490 (Me_3As)[15,19]
ethyl	1	97	420 (Et_3As)[15]
isopropyl	2	94	
tert-butyl	3	91	290 (*t*-$BuAsH_2$)[15]
phenyl		102	490 ($PhAsH_2$)[20]
benzyl	1	78	
allyl	1	77	
triphenylmethyl	3	29	

(1) Kuech, T. F. *Mater. Sci. Rep.* **1987**, *2*, 3.
(2) Stringfellow, G. B. *J. Electron. Mater.* **1988**, *17*, 327.
(3) Lum, R. M.; Klingert, J. K.; Lamont, M. G. *J. Cryst. Growth* **1988**, *89*, 137.
(4) Lum, R. M.; Klingert, J. K.; Kisker, D. W. *J. Appl. Phys.* **1989**, *66*, 652.
(5) Kuo, C. P.; Cohen, R. M.; Stringfellow, G. B. *J. Cryst. Growth* **1983**, *64*, 461.
(6) Speckman, D. M.; Wendt, J. P. *Appl. Phys. Lett.* **1987**, *50*, 676.
(7) Bhat, R.; Koza, M. A.; Skromme, B. J. *Appl. Phys. Lett.* **1987**, *50*, 1194.
(8) Chen, C. H.; Larsen, C. A.; Stringfellow, G. B. *Appl. Phys. Lett.* **1987**, *50*, 218.
(9) Lum, R. M.; Klingert, J. K.; Lamont, M. G. *Appl. Phys. Lett.* **1987**, *50*, 284.
(10) Brauers, A.; Kayser, O.; Kall, R.; Heinecke, H.; Balk, P.; Hoffman, H. *J. Cryst. Growth* **1988**, *93*, 7.
(11) Shastry, S. K.; Zemon, S.; Kenneson, D. G.; Lampert, G. *Appl. Phys. Lett.* **1988**, *52*, 150.
(12) Haacke, G.; Watkins, S. P.; Burkhard, H. *Appl. Phys. Lett.* **1989**, *54*, 2029.

† Present address: Sandia National Laboratories, Albuquerque, NM 87185.
‡ Present address: Department of Chemical Engineering, MIT, Cambridge, MA 02139.
* Author to whom correspondence should be addressed.

0897-4756/90/2802-0039$02.50/0 © 1990 American Chemical Society

Thus, unfortunately, the general trend in reported data for organometallic As is increased film purity with numbers of As–H at the expense of increased toxicity.

The structure of the substituted organic ligands has a strong effect on the behavior of the organometallic arsines. It is desirable that the bond between the arsenic atom and its organic ligands be weak. Organometallic arsenic compounds are likely to decompose via homolytic fission of the carbon–arsenic bond,[13] but alternative mechanisms involving intramolecular reactions have also been proposed.[14,15] Since the bond strengths of most arsenic precursors are unknown, the most effective measure is the stability of the radicals that would form upon carbon–arsenic bond cleavage. The stability of these radicals is expected to correlate closely with the As–C bond strength: the more stable the radical, the weaker the bond. The radical–hydrogen bond strengths, shown in Table II, reflect Markovnikov's rule[20] wherein the hydrogen–carbon bond strength of alkanes increases with the degree of substitution on the α-carbon. That is, relative to the alkane from which each is formed, the order of stability (and ease of formation) of free radicals is

$$3° > 2° > 1° > \text{Me}$$

Table II also demonstrates that the (C–H) bond strength correlates well with the decomposition temperature as measured by molecular beam mass spectroscopy. The decomposition temperature is here taken as the temperature where 50% of the source is reacted. The low C–H bonding energy for the benzyl and allyl radicals, due to their resonance stabilization,[20] makes them possible candidates as ligands for organometallic arsenic sources. For low-temperature growth it would be interesting to examine (triphenylmethyl)arsine, which upon dissociating, would form the triphenylmethyl radical, which is very stable and would not be expected to incorporate carbon.

Other factors of importance when comparing organometallic arsenic sources include vapor pressure and adduct formation. Adduct formation is undesirable if it leads to parasitic gas-phase reactions that result in the depletion of one or both precursors from the gas phase or if it causes enhanced impurity incorporation. An example of this is the reaction between arsine and trimethylindium making an adduct followed by the rapid elimination of hydrocarbons to form an involatile polymer.[21] Volatile adducts, if stable, have been used as precursors.[22–26] The use of adducts, such as Me_3In–PEt_3,[23,26] overcomes problems with prereactions. Moreover, it is possible to purify the adducts to a very high degree by using efficient processes such as zone refining.[23,27] In addition, the adducts tend to be less sensitive to handling than the alloys.[25] Further strengthening of the III/V bond in these compounds has led to single-source precursors for III–V compound semiconductors.[28]

Table III. Gas-Phase Basicities for Group V Hydrides and Their Methyl Derivatives[25] (kcal/mol)

NH_3	201.0	PH_3	187.2	AsH_3	180.7
$MeNH_2$	209.9	$MePH_2$	200.9	$MeAsH_2$	
Me_2NH	216.1	Me_2PH	212.5	Me_2AsH	
Me_3N	220.2	Me_3P	221.4	Me_3As	209.3

The creation of an adduct complex through a reaction such as

$$Me_3As + Me_3Ga \rightarrow Me_3As{:}GaMe_3 \quad (1)$$

depends on the Lewis acid and base characterization of compounds. The negatively charged lone pair of arsines makes them act as Lewis bases, able to bond and react with the Lewis acidic gallium precursors. The Lewis basicity of the alkylarsines is enhanced by the electron-donating nature of their saturated hydrocarbon ligands. The electron-releasing induction of an alkyl group increases with the degree of substitution of its α-carbon. This effect can be readily seen by comparing the relative stability of the carbonium (positive) ions of methane (332 kcal/mol), ethane (299 kcal/mol), and isobutane (262 kcal/mol).[20] The *tert*-butyl carbonium ion is 70 kcal/mol more stable than the methyl carbonium ion, thus the *tert*-butyl group, while being desirable in terms of its low carbon–arsenic bonding energy, can be expected to be a stronger adduct promoter than the less desirable methyl group. A review of the general concepts involved in predicting adduct stability is given by Drago[29] and Purcell and Katz.[30] In the following we briefly summarize reported observations of adducts and growth of GaAs for common arsenic precursors.

The gas-phase Lewis basicity (proton affinity) of trimethylarsene has been measured through the use of ion cyclotron resonance spectroscopy by Hodges and Beauchamp,[31] who compared Me_3As with several other bases as shown in Table III. The gas-phase basicity of the group V hydrides and their methyl derivatives increases with successive methyl substitution corresponding to an increased tendency to form adduct compounds compared to arsine. The formation of an adduct between Me_3Ga and Me_3As has been confirmed by Coates[32] and by Leib et al.,[33] who found its enthalpy of formation to be 10 kcal/mol. The vapor pressure of the adduct was determined by Coates[32] to be

$$\log P(\text{Torr}) = -2458/T + 9.114 \quad (2)$$

which is 6.1 Torr at room temperature (as compared to 181 and 293 Torr for Me_3Ga and Me_3As, respectively). Thus, the adduct would be expected to condense on the reactor walls under some MOCVD growth conditions. Adduct formation between other alkylarsine sources, e.g., Et_3As and t-$BuAsH_2$, and common gallium sources, Me_3Ga and Et_3Ga, is expected to behave analogously.

(13) Lee, P. W.; Omsted, T. R.; McKenna, D. R.; Jensen, K. F. *J. Cryst. Growth* **1988**, *93*, 29.
(14) Larsen, C. A.; Li, B. H.; Buchan, N. I.; Stringfellow, G. B. *J. Cryst. Growth* **1989**, *94*, 673.
(15) Marking, R.; Gladfelter, W. L.; Jensen, K. F. *Chem. Mater.*, submitted.
(16) Morrison, R. T.; Boyd, R. N. *Organic Chemistry*; Allyn and Bacon: Boston, 1966.
(17) Den Baars, S. P.; Maa, B. Y.; Dapkus, P. D.; Danner, A. D.; Lee, H. C. *J. Cryst. Growth* **1986**, *77*, 188.
(18) Lee, P. W.; Omstead, T. R.; McKenna, D. R.; Jensen, K. F. *J. Cryst. Growth* **1987**, *85*, 165.
(19) Omstead, T. R.; Brandon, S.; Hoveland, M. M.; Jensen, K. F. *Mater. Res. Soc. Symp. Ser.*, in press.
(20) Kemp, D. S.; Vellaccio, F. *Organic Chemistry*; Worth Publishers: New York, 1980.
(21) Baliga, B. J.; Ghandhi, S. K. *J. Electrochem. Soc.* **1974**, *121*, 1646.
(22) Maury, F.; El Hammadi, A. *J. Cryst. Growth* **1988**, *91*, 105.
(23) Moss, R. H. *J. Cryst. Growth* **1984**, *68*, 78.
(24) Jones, A. C.; Roberts, J. S.; Wright, P. J.; Oliver, P. E.; Cockayne, B. *Chemtronix* **1988**, *3*, 152.
(25) Bradley, D. C.; Factor, M. M.; Frizo, D. M.; Smith, L. M. *J. Cryst. Growth* **1988**, *92*, 37.
(26) Strubel, K.; Scholz, F.; Laube, G.; Dieter, R. J.; Zielinski, E.; Keppler, F. *J. Cryst. Growth* **1988**, *93*, 347.
(27) Laube, G.; Kohler, U.; Widlein, J.; Scholz, F.; Streuled, K.; Ricter, R. J.; Karl, N.; Gerden, M. *J. Cryst. Growth* **1988**, *93*, 45.
(28) Cowley, A. H.; Benac, B. L.; Eckerdt, J. G.; Jones, R. A.; Kidd, K. B.; Lee, J. Y.; Miller, J. E. *J. Am. Chem. Soc.* **1988**, *110*, 6248.
(29) Drago, R. S. *Struct. Bonding* **1973**, *15*, 73.
(30) Purcell, K. F.; Katz, J. C. *Inorganic Chemistry*; W. B. Sanders: Philadelphia, 1973; Chapter 5.
(31) Hodges, R. V.; Beauchamp, J. L. *Inorg. Chem.* **1975**, *14*, 2887.
(32) Coates, G. E. *J. Chem. Soc.* **1951**, *2*, 2003.
(33) Leib, A.; Emerson, M. T.; Oliver, J. P. *Inorg. Chem.* **1965**, *4*, 1825.

Evidence for adduct formation with these source combinations has been observed in terms of changes in decomposition temperature of the alkyls and in ligand exchanges.[13] The decomposition temperature of Me_3As is lowered when adding Et_3Ga.[13] High boiling point adducts appear to form between Et_3As and both Me_3Ga and Et_3Ga.[13] When Et_3As and an equal amount of either Me_3Ga or Et_3Ga are mixed, the intensities of the mass spectrometer cracking patterns are reduced to approximately 10% of their original intensity levels, indicating the formation of low-volatility compounds. Further indication of the formation of adducts between Me_3Ga and Et_3As is given by the 100 °C decrease in the pyrolysis temperature of Me_3Ga and a 50 °C decrease in the cracking temperature of Et_3As observed in 1:1 mixtures of these compounds. Indication of adduct formation in 1:1 mixtures of Me_3Ga and t-$BuAsH_2$ appears in the form of a reduction in the Me_3Ga decomposition temperature (from 400 to 320 °C) and by a modification of the t-$BuAsH_2$ decomposition products.[13] The production of arsine from the decomposition of t-$BuAsH_2$ is dramatically reduced by the presence of Me_3Ga, and the formation of methylarsenic (MeAs) is observed. A similar decreases in the pyrolysis temperature observed in mixtures of Me_3Ga and AsH_3 has also been attributed to adduct formation.[34]

The decrease in the pyrolysis temperature relative to the single alkyl behavior could also be explained in terms of surface-catalyzed reactions. However, the data on organometallic arsenic sources cited above were obtained in a MOCVD reactor with molecular beam sampling through the substrate.[13,18] Since this design emphasizes gas-phase reactions and minimizes postsampling reactions, surface reactions are less likely to have contributed to the lower pyrolysis temperatures. Furthermore, the observed ligand exchange would indicate the presence of a III–V complex.

In the following we present growth rate data for MOCVD of GaAs by using different organometallic arsenic sources (Me_3As, Et_3As, t-$BuAsH_2$, and $PhAsH_2$) with either Me_3Ga or Et_3Ga. The data show evidence of adduct-related parasitic reactions, and a model based on gas-phase parasitic reactions combined with surface reaction is shown to be consistent with the observations. We have previously presented a similar model for growth with Me_3Ga and t-$BuAsH_2$.[35] The current model is more accurate by including surface-coverage effects, and it is applied to a wider range of compounds and conditions.

Experimental Section

A radiantly heated, microbalance-equipped MOCVD reactor was employed as the primary means of investigating the growth rate of organometallic arsenic precursors with trimethylgallium (Me_3Ga) and triethylgallium (Et_3Ga). This reactor is shown in Figure 1. It consists of a Cahn microbalance from which a double-side polished GaAs wafer is suspended by a thin molybdenum wire. The wafer is held perpendicular to a 2000-W water- and air-cooled quartz-halogen lamp by a small sample holder made out of a single piece of molybdenum wire. The focus of the elliptical lamp reflector is about 1 in. from the 1.5 cm^2 sample so as to achieve a nearly uniform temperature over the entire sample surface. A molybdenum reflector behind the wafer also helps to increase the heating uniformity.

The GaAs substrates were heavily doped with Zn ($\sim 10^{18}$ cm^{-3}) and 0.5 mm thick to make them absorbing in the near-infrared region, where the lamp had the majority of its power output. The high doping also gave the GaAs wafer a high and constant emissivity in the 4.9–5.5-μm range of our optical pyrometer due to

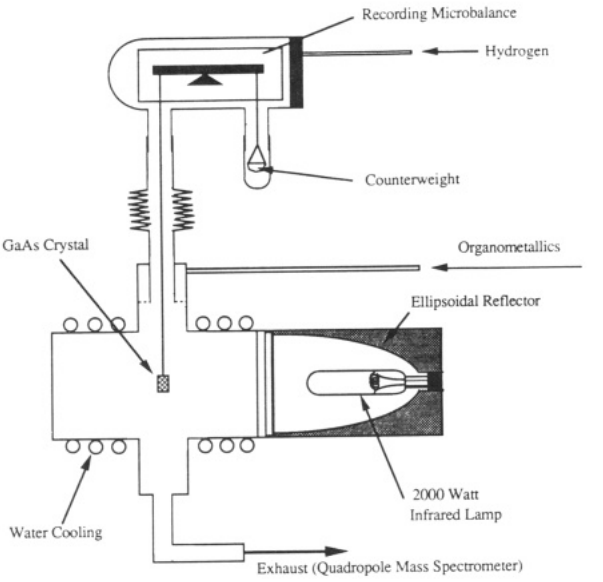

Figure 1. Schematic of a low-pressure MOCVD reactor with a Cahn recording balance for in situ growth rate measurements.

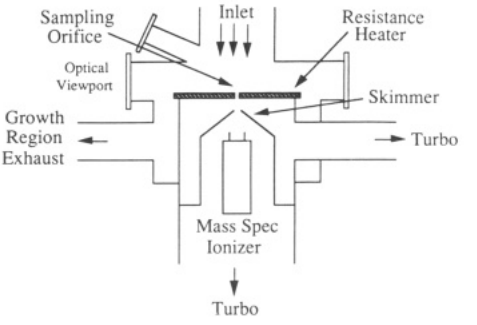

Figure 2. Schematic of a MOCVD reactor with dual-stage sampling through the deposition surface to a Balzer QMS 311 quadrupole mass analyzer.

valence-band transitions.[36] This allowed for accurate temperature measurement in an optical region not interfered with by the radiation from the quartz lamp.

Wafers were degreased and etched before being loaded into the reactor, after which the system was baked and purged overnight before taking data. During experiments the wafer was held at a given temperature for about 10 min to obtain a growth rate measurement, except for conditions with very low growth rates. In those cases, up to 30 min was required to obtain an accurate reading above the noise caused by minor pressure fluctuations in the system. The surface morphology of the sample was monitored, and if it had deteriorated significantly after a set of runs, the data from the entire run were discarded.

The total system pressure was usually kept constant at 1 Torr while the V/III ratio (i.e., moles of arsenic/moles of gallium) was varied between 2 and 20. Typical feed rates of Me_3Ga and Et_3Ga corresponded to 0.01 Torr of partial pressure of the organometallic in the system. Hydrogen flow rates were varied from 30 to 45 sccm to evaluate the effect of residence time. To investigate the effect of adduct formation in the gas lines, the organometallic source compounds were introduced in two different ways. In the first case (combined flow) the gallium and arsenic alkyls were mixed in the gas manifold approximately 5 feet from the reactor. In the second case (split flow) the arsenic source was introduced through the microbalance housing while the gallium source was fed through an annulus directly adjacent to the GaAs wafer.

Films for measurement of electrical properties were deposited by using doped GaAs as a susceptor for a semiinsulating substrate.

A special MOCVD reactor with molecular beam sampling through the susceptor was used to investigate the decomposition of $PhAsH_2$. This system, shown schematically in Figure 2, has

(34) Larsen, C. A.; Buchan, N. I.; Stringfellow, G. B. *Appl. Phys. Lett.* **1988**, *52*, 480.
(35) Omstead, T. R.; Van Sickle, P. M.; Jensen, K. F. *J. Cryst. Growth* **1988**, *93*, 20.
(36) Jordan, A. S. *J. Appl. Phys.* **1980**, *51*, 2218.

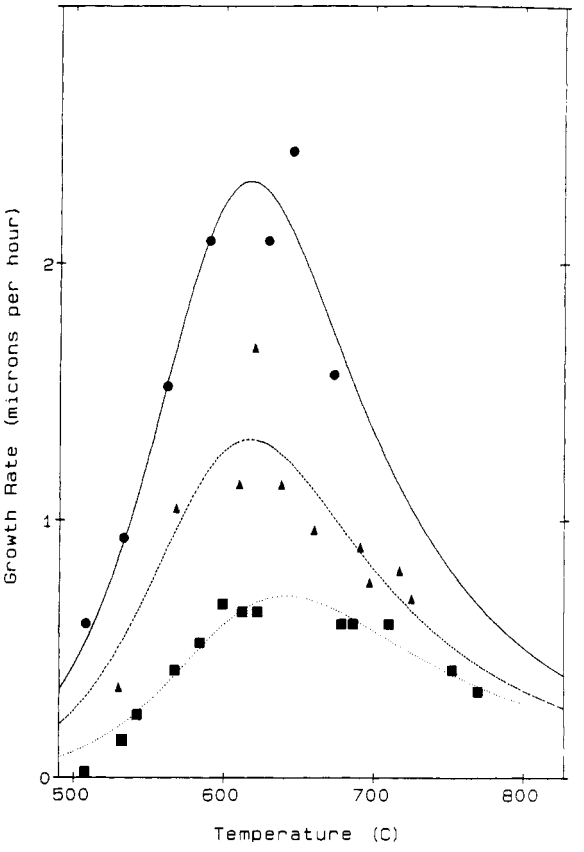

Figure 3. Growth rate of GaAs deposited from Me_3As and Me_3Ga as a function of substrate temperature for different flow rates of the carrier gas (H_2): ■, 30 sccm; ▲, 37.5 sccm; ●, 45 sccm. The solid curves represent model predictions. P_{total} = 1 Torr, P_{Me_3Ga} = 0.01 Torr, V/III = 5.

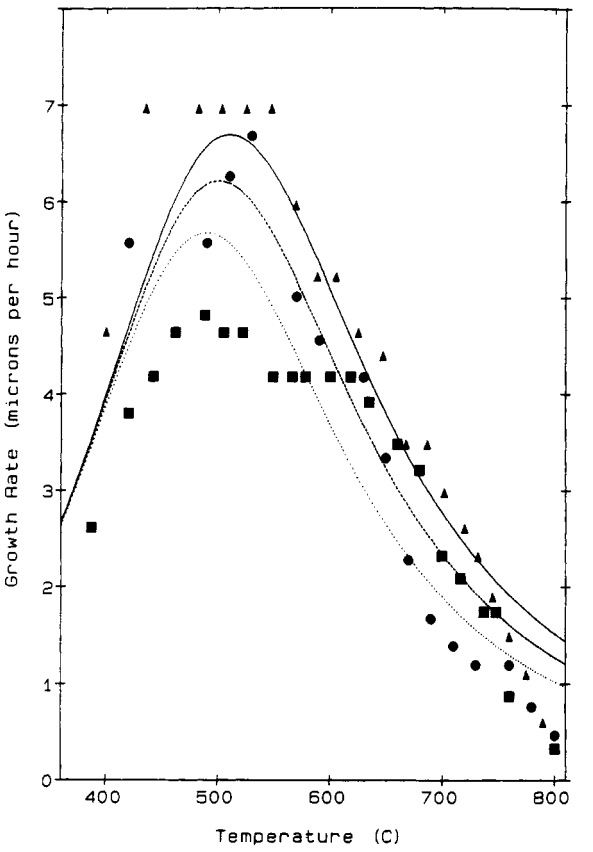

Figure 4. Growth rate of GaAs deposited from Me_3As and Et_3Ga as a function of substrate temperature for different flow rates of the carrier gas (H_2): ■, 30 sccm; ▲, 37.5 sccm; ●, 45 sccm. The solid curves represent model predictions. P_{total} = 1 Torr, P_{Me_3Ga} = 0.01 Torr, V/III = 5.

been described previously.[13,18] The gas was sampled through a 100-μm pinhole in a 25-μm-thick stainless steel foil in the center of a resistively heated graphite susceptor. The sample was expanded into a molecular beam in the two-stage pumping system and directed into a Balzers 311 quadrupole mass spectrometer. This arrangement made it possible to extract a sample just above the growth surface and to analyze it with minimal interactions from past sampling gas-phase and wall reactions. The thermal pyrolysis of $PhAsH_2$ in H_2 was studied with and without the presence of Me_3Ga and Et_3Ga by monitoring the peak intensities as a function of susceptor temperature. The reactor pressure was 20 Torr. A H_2 flow rate of 30 sccm was used, and typical feed rates of the organometallic compounds corresponded to a 1 Torr of partial pressures in the reactor chamber.

Results

Growth of GaAs Using Me_3As with Me_3Ga or Et_3Ga. The kinetics of the growth of GaAs using Me_3Ga and Me_3As was investigated by measuring growth rate as a function of temperature using the microbalance reactor while holding the partial pressure of Me_3Ga and Me_3As constant at 0.01 and 0.05 Torr, respectively. To determine the influence of the gas residence time, three different flow rates were used. The effect of flow rate, or equivalently residence time, on growth with Me_3Ga/Me_3As and Et_3Ga/Me_3As is shown in Figures 3 and 4, respectively. Both graphs show an increase in growth rate with a decrease in residence time, which is indicative of gas-phase depletion. Growth with Et_3Ga/Me_3As was found to be difficult at temperatures below 550 °C because of the formation of gallium droplets. The generation of gallium droplets is probably caused by the large difference in decomposition temperatures of Et_3Ga and Me_3As. Triethylgallium cracks at about 350 °C, while trimethylarsene is observed to decompose significantly only at temperatures above approximately 500 °C.[13,18] The difference in the decomposition temperature between the two compounds leads to a lack of arsenic at the growth surface and gallium droplets result.

Growth of GaAs Using Et_3As with Me_3Ga or Et_3Ga. The effect of total flow rate on the growth of GaAs using Me_3Ga and Et_3As is shown in Figure 5. The growth rate observed by using Me_3Ga and Et_3As, while still low, is larger than that observed by using Me_3Ga and Me_3As. The higher growth rate is probably due to the lower thermal stability of Et_3As as compared to Me_3As, which gives an increased partial pressure of arsenic at the growth surface. Growth using Me_3Ga/Et_3As was also observed to have a strong dependence on residence time, which again is most likely due to the loss of precursor from the gas phase. Growth using Et_3Ga and Et_3As was not achieved under any conditions investigated. The lack of growth when using this combination of precursors may be due to the formation of an involatile adduct compound as evidenced by the observation of a white, polymeric substance on the inlet lines after the mixing point of the two precursors.

Growth of GaAs Using *t*-$BuAsH_2$ with Me_3Ga or Et_3Ga. The kinetic behavior of the $Me_3Ga/tBuAsH_2$ system was investigated by measuring the growth rate as a function of temperature and residence time (total flow rate) in the reactor under the same conditions as the Me_3As and Et_3As studies. The results, shown in Figure 6, show two distinct regions of growth. At low temperatures the deposition rate is independent of the flow rate, which indicates that growth in this regime is controlled by surface (heterogeneous) reactions. In the midtemperature region, at temperatures above 600 °C, a significant

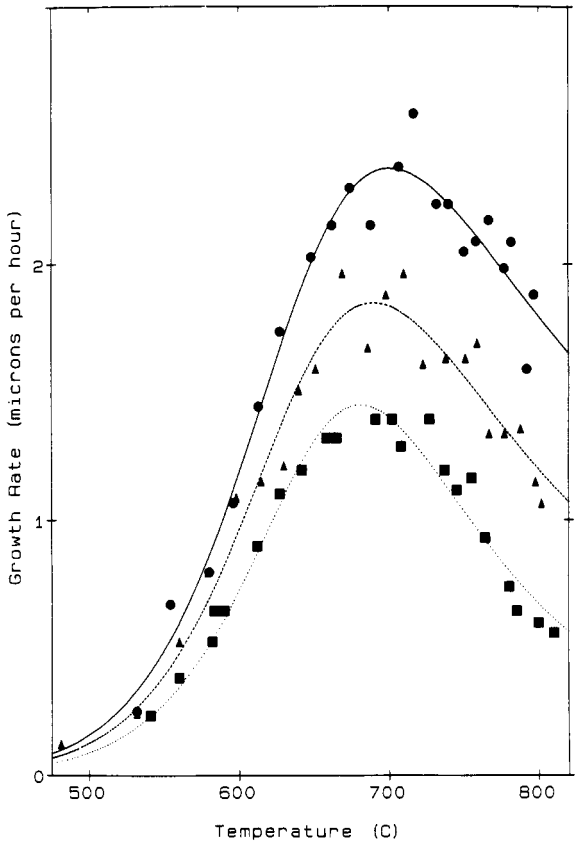

Figure 5. Growth rate of GaAs deposited from Et_3As and Me_3Ga as a function of substrate temperature for different flow rates of the carrier gas (H_2): ■, 30 sccm; ▲, 37.5 sccm; ●, 45 sccm. The solid curves represent model predictions. P_{total} = 1 Torr, P_{Me_3Ga} = 0.01 Torr, V/III = 5.

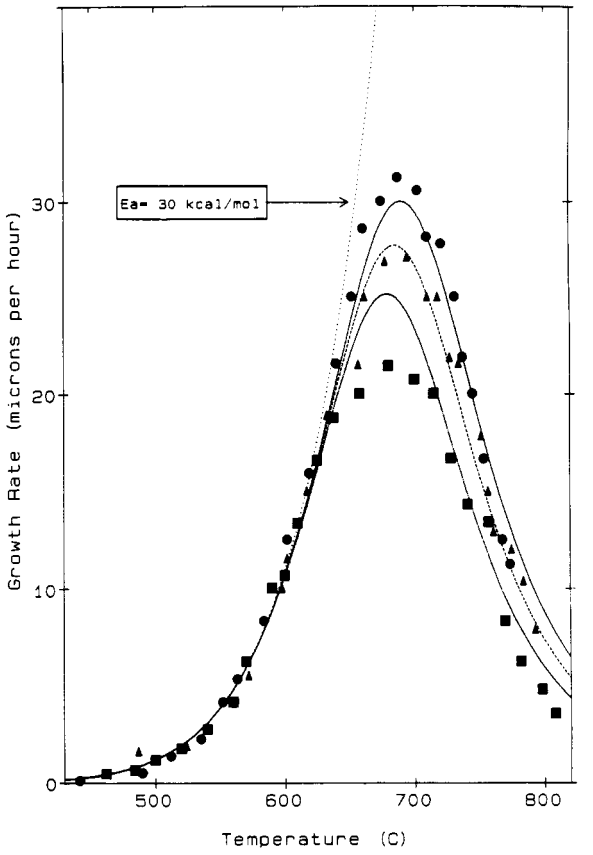

Figure 6. Growth rate of GaAs deposited from $tBuAsH_2$ and Me_3Ga as a function of substrate temperature for different flow rates of the carrier gas (H_2): —, 30 sccm; ▲, 37.5 sccm; ●, 45 sccm. The solid curves represent model predictions. P_{total} = 1 Torr, P_{Me_3Ga} = 0.01 Torr, V/III = 5.

dependence of the growth rate on the total flow rate is observed.

The temperature dependence of the growth rate of GaAs from Et_3Ga and t-$BuAsH_2$ at low pressures is similar to that observed for the Me_3Ga + t-$BuAsH_2$, except that the growth is shifted to lower temperatures, as illustrated in Figure 7. The maximum growth rate occurs around 750 °C for Me_3Ga, while it takes place around 450 °C for Et_3Ga. This is consistent with the larger bond strength of the methyl group as compared to the ethyl compound and the increased general tendency of ethyl-containing precursors to form adducts. The increased degree of parasitic reaction using Et_3Ga/t-$BuAsH_2$ is also evidenced by the extreme effect of residence time or equivalently flow rate on the growth rate. Unlike the situation for Me_3Ga, a surface kinetic controlled regime, where the growth rate is independent of flow rate, is not apparent at low temperatures (<450 °C).

Electrical Properties. To investigate the electrical properties of GaAs films grown by using Et_3Ga and t-$BuAsH_2$ as precursors, which has not been done previously, films were grown on undoped GaAs using doped GaAs as a susceptor in the microbalance reactor. The mobility of the films increases with decreasing pressure as shown in Table IV. This is consistent with the presence of gas-phase reactions which lead to impurity incorporation in the growing film. Lower pressure will reduce gas-phase reactions and consequently minimize contamination. Further evidence of the adverse effect of gas-phase reactions between the precursors is the decrease in film quality with increasing V/III ratio for V/III ratios above 5. This is in contrast to conventional MOCVD with Me_3Ga/AsH_3 at low pressures, where the optimal V/III ratio is typically

Table IV. Electrical Properties of GaAs Grown by Using Et_3Ga/t-$BuAsH_2$

T, °C	P, Torr	V/III	μ(77 K)	type	mobilities, cm²/(V s) μ(300 K)	μ(77 K)
625	1	5	1×10^{16}	n	130	
650	1	3	3×10^{16}	n	1522	
650	1	4	4×10^{16}	n	1952	1913
650	1	5	6×10^{15}	n	4170	7592
650	1	7.5	1×10^{15}	n	1323	1643
650	1	10	3×10^{17}	p	110	187
650	0.5	5	3×10^{15}	n	4000	9700
650	2.5	5	7×10^{15}	n	3633	5683
650	5	5	1×10^{16}	n		4143

very high.[1] The best film, grown at a pressure of 0.5 Torr, a V/III ratio of 5, and a temperature of 650 °C, has a 77 K mobility of 9700 cm²/(V s). This is the lowest pressure investigated, and it is likely that even cleaner films could be achieved at lower pressures. However, the current experimental arrangement makes it difficult to grow at lower pressures. A photoluminescence spectrum of this film (Figure 8) is characterized by donor- or acceptor-bound excitons (D or A,X) at short wavelengths and by free electron to acceptor [(e,C^0) and (e,Zn^0)] as well as donor to acceptor transitions (D^0, Zn^0) at longer wavelengths. These transitions indicate the presence of carbon and zinc impurities.[1] Carbon incorporationis related to the growth process, while zinc is present in the doped wafer used as a susceptor. Thus, autodoping appears to be a problem affecting the quality of our films. The nature of the n-type impurity making the films n-type overall has not been determined. Nevertheless, the combination of Et_3Ga and t-$BuAsH_2$ as GaAs precursors deserves further investigation in a system specifically designed to produce

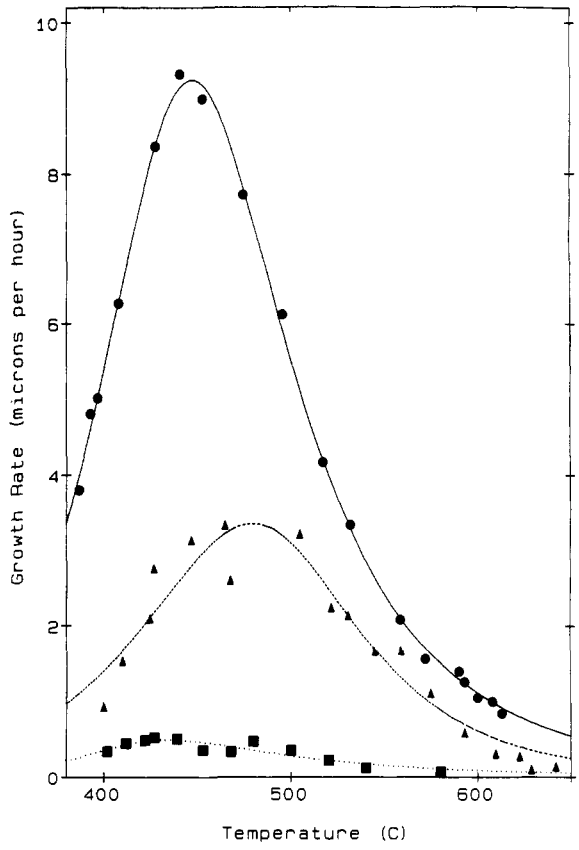

Figure 7. Growth rate of GaAs deposited from t-$BuAsH_2$ and Et_3Ga as a function of substrate temperature for different flow rates of the carrier gas (H_2): ■, 30 sccm; ▲, 37.5 sccm; ●, 45 sccm. The solid curves represent model predictions. P_{total} = 4 Torr, P_{Me_3Ga} = 0.01 Torr, V/III = 5.

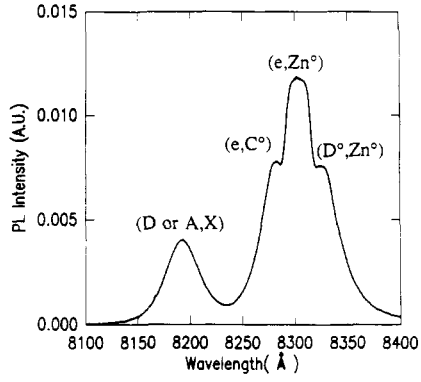

Figure 8. The 9 K photoluminescence spectrum of GaAs film grown from t-$BuAsH_2$ and Et_3Ga at 0.5 Torr and 650 °C. P_{total} = 0.5 Torr, P_{Et_3Ga} = 0.01 Torr, V/III = 5.

films with good electrical and optical properties.

Growth of GaAs Using $PhAsH_2$ and Me_3Ga or Et_3Ga. This precursor has already been demonstrated to be capable of producing high-quality GaAs.[10] It is an attractive alternative to *tert*-butylarsine (t-$BuAsH_2$) since the delocalizing effect of its phenyl ligand is expected to make it less likely than t-$BuAsH_2$ to prereact with gallium sources and dopants. To investigate the gas-phase interactions of phenylarsine with gallium species, a decomposition study was performed with and without the presence of Me_3Ga or Et_3Ga. The results, shown in Figure 9, demonstrate that although there is some enhancement of the $PhAsH_2$ cracking rate due to the presence of gallium precursors, it is much less severe than for the case of t-$BuAsH_2$.[13] Both Me_3Ga and Et_3Ga have essentially the same effect, enhancing the rate of gas-phase cracking without significantly altering its onset.

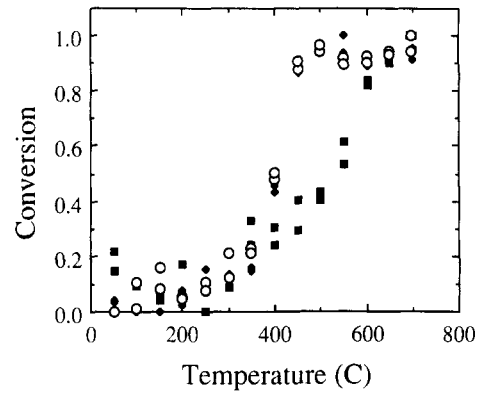

Figure 9. Conversion of $PhAsH_2$ in H_2 as a function of substrate temperature and feed composition (■, $PhAsH_2$; ○, Me_3Ga + $PhAsH_2$; ●, Et_3Ga + $PhAsH_2$). $P_{total} \approx 20$ Torr, P_{PhAsH_2} = 1 Torr, V/III = 1.

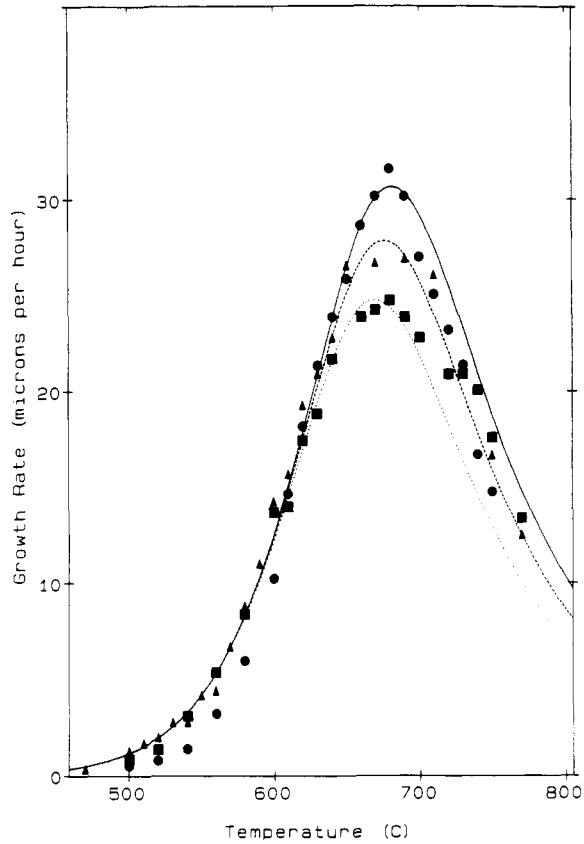

Figure 10. Growth rate of GaAs deposited from $PhAsH_2$ and Me_3Ga as a function of substrate temperature for different flow rates of the carrier gas (H_2): ■, 30 sccm; ▲, 37.5 sccm; ●, 45 sccm. The solid curves represent model predictions. P_{total} = 1 Torr, P_{Me_3Ga} = 0.01 Torr, V/III = 5.

To further investigate the role of parasitic reactions in growth with Me_3Ga and $PhAsH_2$, the microbalance reactor was used to determine the growth rate at different temperatures and at flow rates (Figure 10) under conditions identical with those used in studying t-$BuAsH_2$. The difference in the growth rate at various flow rates is related to a combination of parasitic reactions and depletion effects from deposition. A comparison of these data with those obtained for t-$BuAsH_2$ shows that the effect of parasitic reactions is slightly smaller for $PhAsH_2$ than for t-$BuAsH_2$. In the case of t-$BuAsH_2$ the maximum growth rate varies from 22 to 31 μm/h with an increase in flow

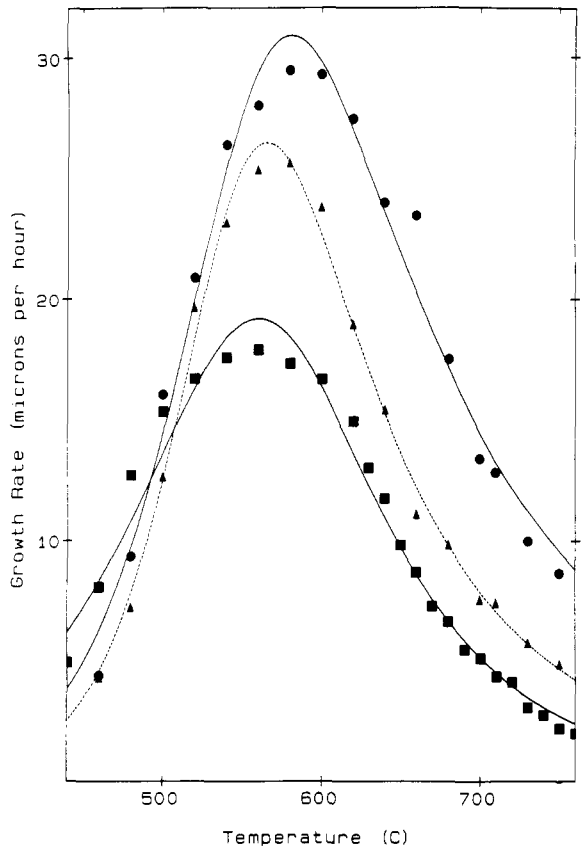

Figure 11. Growth rate of GaAs deposited from $PhAsH_2$ and Et_3Ga as a function of substrate temperature for different flow rates of the carrier gas (H_2): ■, 30 sccm; ▲, 37.5 sccm; ●, 45 sccm. The solid curves represent model predictions. P_{total} = 1 Torr, P_{Me_3Ga} = 0.01 Torr, V/III = 5.

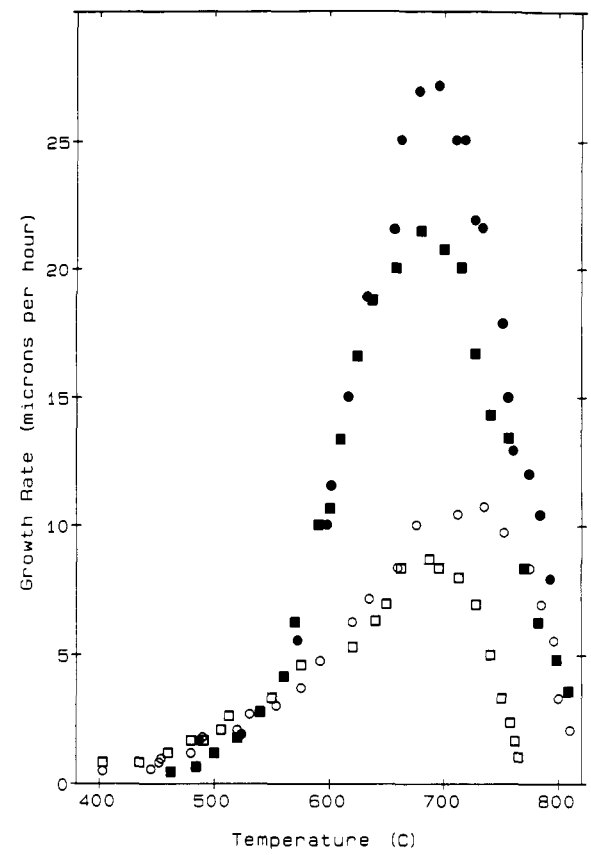

Figure 12. Growth rate of GaAs deposited from Me_3Ga and t-$BuAsH_2$ as a function of substrate temperature and H_2 carrier gas flow rate for split streams (solid points) and combined streams (open points): ■, 30 sccm; ●, 37.5 sccm; P_{total} = 1 Torr, P_{Me_3Ga} = 0.01 Torr, V/III = 5.

rate from 30 to 45 sccm (cf. Figure 6), while this variation is reduced to 25 to 31 μm/h when $PhAsH_2$ is used. The slightly higher growth rate with $PhAsH_2$ at the low flow rates relative to t-$BuAsH_2$ is further evidence for less parasitic gas-phase reactions. Growth using Et_3Ga/$PhAsH_2$ (Figure 11) is far less affected by parasitic reactions than with Et_3Ga/t-$BuAsH_2$, with the maximum growth rate occurring at approximately 150 °C higher temperature, and flow effects being far less important. In the case of $PhAsH_2$ the maximum growth rate varies only from 30 to 19 μm/h when the flow rate is reduced from 45 to 30 sccm. On the other hand, the maximum growth rate varies from 9.2 to 0.5 μm/h when t-$BuAsH_2$ is the arsenic source (cf. Figure 7).

Discussion

Two possible mechanisms for the dependence of growth rate on flow rate may be proposed. The first, mass-transfer limitation, is unlikely due to the high diffusivity of the gallium precursors at 1 Torr (~350 cm^2/s). A simple analysis of the reactor shows that mass transfer is primarily accomplished by Fickian diffusion from a large volume that may be considered to be well mixed because of the high diffusivities of the precursor. Free-convection-induced recirculations are also expected to be negligible since the Grashof number (a measure of the strength of the natural convection[37]) is very small (≈1) at this pressure. Calculations assuming diffusion-limited growth predict growth rates an order of magnitude higher than those experimentally observed.

A more likely explanation for the observed growth-rate dependence on flow rates is gas-phase depletion caused by parasitic reactions. The growth efficiency (moles of gallium in the growing film/moles entering the reactor) is high (41% at 700 °C), and thus the loss of precursor from the gas phase will directly affect the growth rate. In Figure 12 a comparison of growth with split and combined feed streams is shown. The growth rate is noticeably lower when the reagents are combined upstream of the reactor than when they are combined inside the reactor (split stream). This difference in the growth rate between split and combined feed streams suggests that a parasitic reaction occurs, and that this reaction is related to adduct formation in the lines. Since the growth rates for split and combined streams are nearly equal at low temperatures, the parasitic reaction does not take place in the lines but requires higher temperatures to occur. This suggests that the experimental observations can be explained by a model based on the reversible formation of an adduct and the decomposition of this adduct to useless polymeric material competing with the growth of GaAs. This simplified mechanism takes the form

$$\text{GaAs} \xleftarrow{k_s} \text{organometallic precursors} \underset{k_r}{\overset{k_f}{\rightleftharpoons}} \text{adduct} \xrightarrow[k_d]{} \text{polymeric deposits} \quad (3)$$

Here k_f and k_r are the forward and reverse rate constants for adduct formation, respectively, k_d is the rate constant for the irreversible decomposition of the adduct to polymer, and k_s is the surface reaction rate constant for the growth of GaAs. Each step obviously involves several elementary reactions, but there are insufficient data to provide additional mechanistic detail at this stage. Be-

(37) Bird, R. B.; Stewart, W. E.; Lightfoot, E. N. *Transport Phenomena*; Wiley: New York, 1960.

cause of the low pressures (i.e., large diffusion coefficients), the hot reaction zone around the substrate may be considered to be a "well-mixed reactor" with residence time τ = (volume/volumetric flow rate). A steady-state balance over the gallium alkyl then takes the form

$$P_{G0} - P_G - \tau k_f P_G P_A + \tau k_r P_C - \tau(S/V)R_{surface} = 0 \quad (4)$$

Here P_A, P_G, and P_C represent the partial pressures of the arsenic precursor, the gallium precursor, and the adduct complex, respectively. S is the surface area, and $R_{surface}$ is the surface reaction rate. The subscript 0 refers to inlet conditions. V is the reactor volume. The first two terms give the difference between gallium precursor in- and outflow in the reacting gas volume. The next two terms represent the net reversible formation of adduct, while the last term gives the loss of gallium alkyl in deposition reactions. A similar balance over the adduct complex (C) gives

$$P_{C0} - P_C + \tau k_f P_G P_A - \tau k_r P_C - \tau k_d P_C = 0 \quad (5)$$

The first term represents the partial pressure of adduct formed in the gas-handling system. For the case of a low boiling adduct as in the Et_3Ga experiments or split streams as in the Me_3Ga experiments this term is essentially zero. Since the activation energy for adduct formation is small, we can assume that k_r is much larger than k_d, and we have

$$P_C = \frac{\tau k_f P_G P_A}{[1 + \tau k_r + \tau k_d]} \simeq \frac{k_f P_G P_A}{k_r} = K_c P_G P_A \quad (6)$$

On the basis of observations for atomic layer epitaxy and recent surface studies,[38-40] the surface reactions of Ga species appear to be self-limiting. Therefore, we assume that the growth rate follows a simple bimolecular, separate-sites Langmuir–Hinshelwood mechanism:

$$R_{surface} = \frac{k_s K_G K_A P_G P_A}{[1 + K_G P_G][1 + K_A P_A]} \quad (7)$$

where K_G and K_A are the adsorption equilibrium constants for surface gallium and arsenic species, respectively. k_s is the surface reaction rate constant. For large V/III ratios the surface reaction will be saturated with adsorbed arsenic species, i.e., $1 \ll K_A P_A$, and P_A is approximately equal to the inlet partial pressure P_{A0}. At high temperatures, where gas-phase parasitic reactions are important, gallium surface coverages are low and the Langmuir–Hinshelwood expression then reduces to

$$R_{surface} = k_s K_G P_G \quad (8)$$

The unknown partial pressure of gallium in the reactor P_G can then be determined by inserting eq 8 into eq 4 and solving eq 4–6 simultaneously for P_G. Since the residence time, τ, is inversely proportional to the flow rate, F, one then obtains the following simplified expression for the growth rate as a function of H_2 carrier gas flow rate (F) and temperature (T) through the temperature dependence of the rate constants:

$$R_{surface} = \frac{k'_s k_1 F P_{G0}}{1 + F k_1} \quad (9)$$

where the quantities

$$k'_s = k_s K_G \quad (10)$$

$$k_1 = 1/[k_d K_C P_A V + k_s S K_G] \quad (11)$$

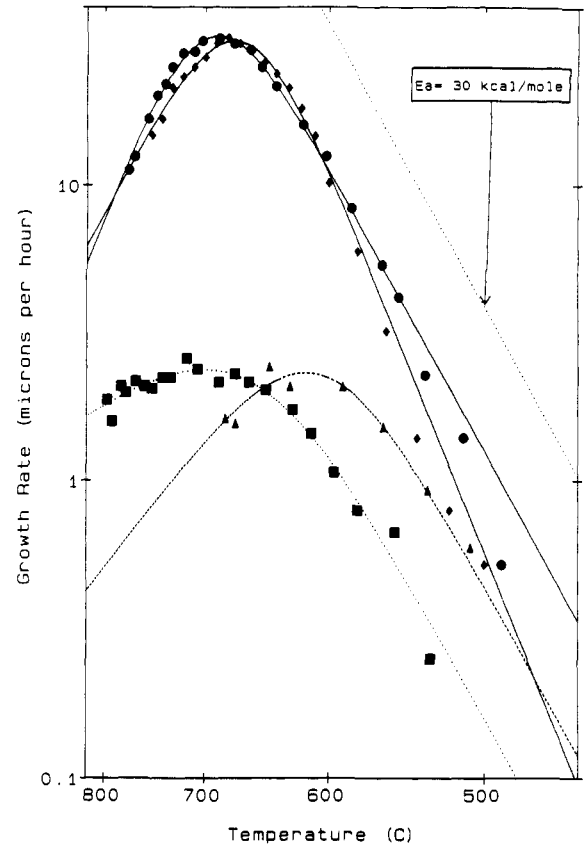

Figure 13. Growth rates of GaAs deposited from Me_3Ga with Me_3As (▲), Et_3As (■), t-$BuAsH_2$ (●), and $PhAsH_2$ (◆) as a function of $1/T$(K). Note: for convenience the growth temperature in °C is shown on the abcissa rather than $1/T$ (P_{total} = 1 Torr, P_{Me_3Ga} = 0.01 Torr, V/III = 5, flow rate = 45 sccm).

represent loss of precursor from the gas phase by film growth and by parasitic reaction. From independent measurements of k_s and k_G, to be discussed in more detail later, it was found that at high temperatures $k_d K_c P_A V \gg k_s S K_G$, which implies that

$$k_1 \simeq \frac{1}{k_d K_C P_A V} \quad (12)$$

The temperature dependence of the constants k'_s and k_1 is given by the Arrhenius form

$$k'_s = k'_{s0} e^{-E'_{As}/RT} \qquad k_1 = k_{10} e^{-E_{A1}/RT} \quad (13)$$

where k'_{s0} and k_{10} are the preexponential factors of E_{As} and E_{A1} represent the activation energies. The unknown rate parameters (k'_{s0}, E'_{As}, k_{10}, and E_{A1}) are determined by nonlinear regression of the deposition model, eq 9, to the measured growth rates as a function of substrate temperatures and flow rates. The model predictions are shown as solid lines in Figures 3–7 and 10–11. The agreement with the data is very good except in the case of Et_3Ga/Me_3As, where the formation of gallium droplets occurs.

The determined rate parameters are summarized in Table V. Because of the gallium droplet formation in the source combination Et_3Ga/Me_3As, no rate parameters are reported for that case. Comparison of the rate constants shows that within experimental error the activation energies of the surface reactions (E'_{As}) are the same within the group of experiments performed with Me_3Ga (~30 kcal/mol) and within the experiments with Et_3Ga (~24 kcal/mol). This is further demonstrated in Figure 13, which shows similar slopes for the reaction curves for Me_3Ga with the different arsenic sources except for

(38) Nishizawa, J.; Kurabayashi, T.; Abe, H. *Surf. Sci.* **1987**, *185*, 249.
(39) Den Baars, S. P.; Dapkus, P. D.; Beyler, C. A.; Hariz, A.; Dzurko, *J. Cryst. Growth* **1988**, *93*, 195.
(40) Aspnes, D. E.; Colas, E.; Studna, A. A.; Bhat, R.; Koza, M. A.; Keramidas, V. G. *Phys. Rev. Lett.* **1988**, *61*, 2702.

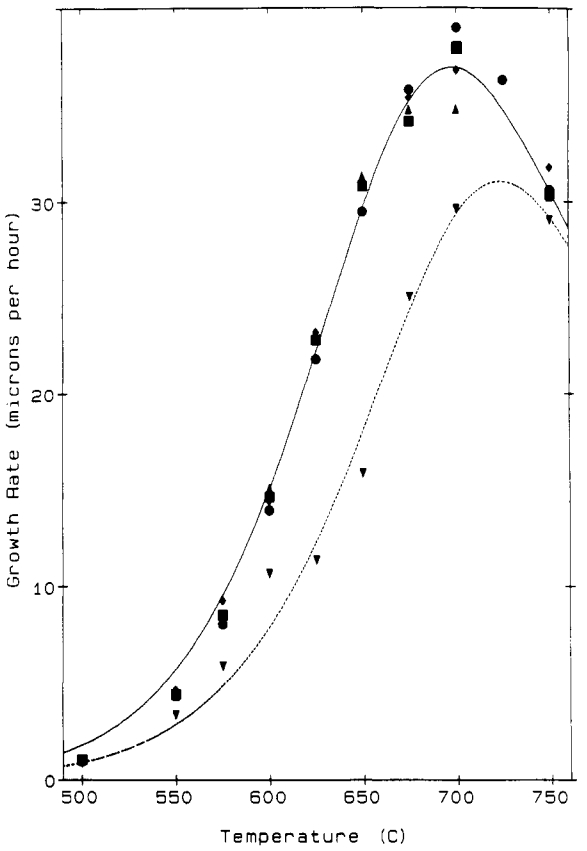

Figure 14. Growth rate of GaAs deposited from t-$BuAsH_2$ and Me_3Ga for differential partial pressures of t-$BuAsH_2$ and temperatures: ▼, $P_{t\text{-}BuAsH_2}$ = 0.02 Torr; ◆, $P_{t\text{-}BuAsH_2}$ = 0.035 Torr; ▲, $P_{t\text{-}BuAsH_2}$ = 0.067 Torr; ■, $P_{t\text{-}BuAsH_2}$ = 0.085 Torr; ●, $P_{t\text{-}BuAsH_2}$ = 0.1 Torr; P_{total} = 1 Torr, P_{Me_3Ga} = 0.01 Torr.

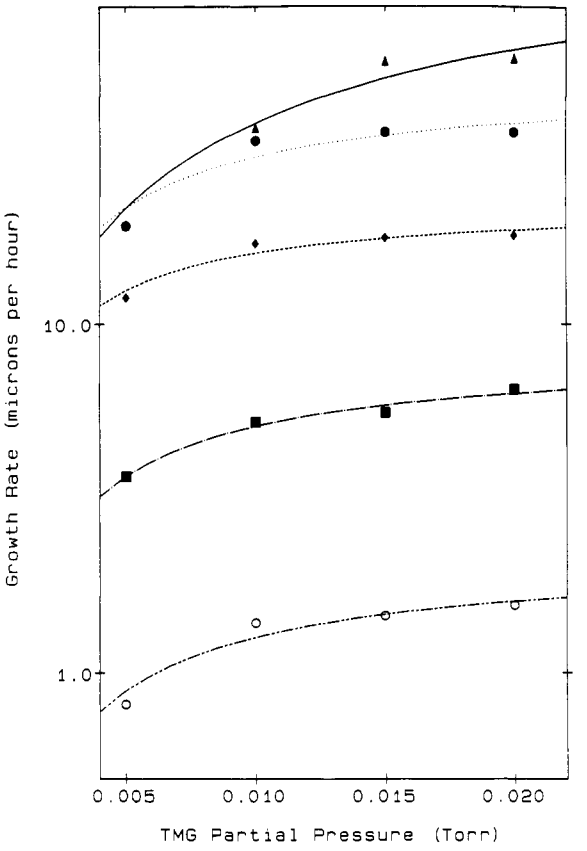

Figure 15. Growth rate of GaAs deposited from t-$BuAsH_2$ and Me_3Ga as a function of Me_3Ga partial pressure for different temperatures: ○, 500 °C; ■, 550 °C; ◆, 600 °C; ●, 650 °C; ▲, 700 °C. P_{total} = 1 Torr, V/III = 5.

$PhAsH_2$. This supports the model assumption of arsenic being in excess so that only the adsorption characteristics of the gallium species are important. This will be discussed further below. The lower activation energy when using Et_3Ga as compared to Me_3Ga is also consistent with the relative bond strengths of the carbon–gallium bond in the two components.[41,42]

The model contains four unknown rate parameters (two preexponential factors and two activation energies) which have been determined by nonlinear least-squares regression on the data. This raises the question whether or not other models with two rate constants could be made to fit the data. However, the excellent agreement obtained with a large amount of data for several different compounds and over a range of processing conditions, combined with the prediction of known bond strength trends, strongly supports this model. Thus, the interpretation that the growth is governed by surface reactions at low temperature and by parasitic gas-phase reactions at high temperature is consistent with the experimental observations.

The composite rate constant k_1 involves contributions from the irreversible decomposition of the adduct (k_d) and the equilibrium constant for the adduct (K_c). From eq 12 we find that $E_d = -E_{A1} - \Delta H_{adduct}$. Since the heat of formation of adducts typically is low ($-\Delta H_{adduct} \sim 10$ kcal/mol),[43] variations in E_{A1} primarily reflect the decomposition reaction to polymeric material. Comparison of the values for t-$BuAsH_2$ and $PhAsH_2$ again show lower activation energies for the Et_3Ga cases than for Me_3Ga, indicating that elimination from the ethyl-based adducts is more facile. Furthermore, the rate constant for Et_3Ga/$PhAsH_2$ is much less than that for Et_3Ga/t-$BuAsH_2$ (0.07 vs 7.1 mol/s at 700 °C), in agreement with the data showing less variation in the maximum growth rate with flow rate (i.e., less parasitic reaction) for the Et_3Ga/$PhAsH_2$ source combination.

The model relies on the assumption that As species are in excess, so that the adsorption of arsenic is saturated. This assumption is supported by the growth rate variation with the partial pressure of t-$BuAsH_2$ displayed in Figure 14. For partial pressures of t-$BuAsH_2$ above 0.035 Torr, corresponding to a V/III ratio of 3.5, the growth rate is essentially independent of partial pressure of t-$BuAsH_2$. Since the above discussion has focused on data obtained for V/III = 5, the assumption is reasonable. However, for low V/III ratios it will be necessary to use a more complex model than the one presented.

The existence of a surface reaction controlled region for growth temperatures below 600 °C for Me_3Ga and the activation energy, E'_{As}, being independent of the arsenic source (cf. Table V and Figure 13) indicate that the surface reactions of Me_3Ga-related species control growth. This makes it possible to independently evaluate the surface reaction rate constant, k_s, and the adsorption constant, K_G, which are lumped together in the expression for k'_s, eq 10. Since the arsenic adsorption is saturated, and gas-phase depletion is not important at low temperatures, the surface reaction expression (eq 7) reduces to the following simple Langmuir–Hinshelwood form:

$$R_{surface} = \frac{k_s K_G P_G}{[1 + K_G P_G]} \qquad (14)$$

(41) Paputa, M. C.; Price, S. J. W. *Can. J. Chem.* **1979**, *57*, 3178.
(42) Jacko, M. G.; Price, S. J. W. *Can. J. Chem.* **1963**, *4*, 1560.
(43) Tirtowidjojo, M.; Pollard, R. *J. Cryst. Growth* **1986**, *77*, 200.

Table V. Rate Parameters Determined by the Fit of the Kinetic Model, Eq 9, to the Experimental Data

	Figure	k'_{s0}, cm/(Torr s)	E'_{As}, kcal/mol	k_{10}, mol/s	E_{A1}, kcal/mol
Me_3Ga/Me_3As	3	130 ± 20	29.4 ± 1	(2 ± 5) × 10^9	−48.7 ± 5
Me_3Ga/Et_3As	5	70 ± 20	29.4 ± 1	(8 ± 5) × 10^7	−45.6 ± 5
$Me_3Ga/tBuAsH_2$	6	690 ± 20	29.4 ± 1	(3 ± 5)× 10^{12}	−67.2 ± 5
$Me_3Ga/PhAsH_2$	9	4600 ± 10	32 ± 5	(3 ± 5) × 10^{11}	−61.7 ± 5
$Et_3Ga/tBuAsH_2$	6	170 ± 20	23.4 ± 5	(1.3 ± 5) × 10^{11}	−45.7 ± 5
$Et_3Ga/PhAsH_2$	10	233 ± 20	23.9 ± 1	9.6 × 10^8	−45.1 ± 5

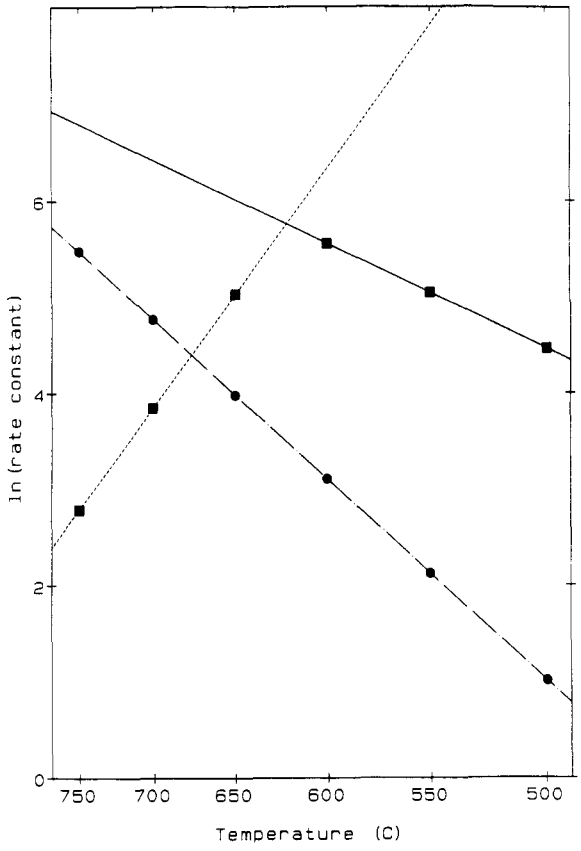

Figure 16. Arrhenius plots of the surface rate constant k_s and the Me_3Ga adsorption constant K_G, based on a fit of eq 14 to data in Figure 14. Note: for convenience the growth temperature in °C is shown on the abcissa rather than $1/T$.

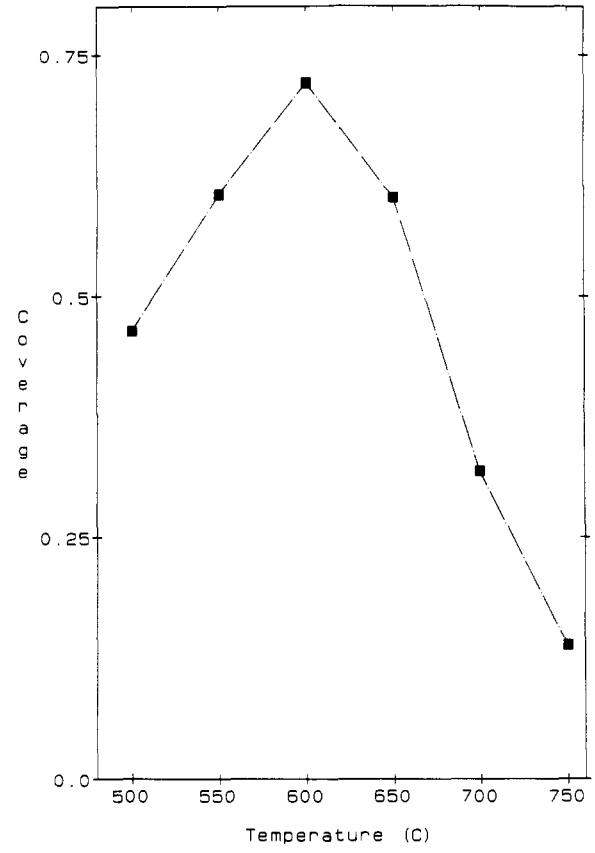

Figure 17. Predicted surface coverage of gallium species as a function of temperature for base conditions, P_{total} = 1 Torr, P_{Me_3Ga} = 0.01, V/III = 5.

This approach of dividing the growth into two regimes simplifies the overall rate expressions to a tractable form and works well for the case of Me_3Ga/t-$BuAsH_2$, where the separate regions are easily identifiable.

To obtain k_s and K_G, the simplified Langmuir–Hinshelwood expression (eq 14) is fit to growth rate data for varying partial pressures of Me_3Ga at a variety of temperatures as shown in Figure 15. The curves obtained in the surface controlled region ($T \leq 600$ °C) are well described by Langmuir–Hinshelwood kinetics, giving the temperature dependence of k_s and K_G shown in Figure 16. The determined rate and adsorption constants are

$$k_s = (2.3 \times 10^8\ \mu\text{m/h}) \exp\left(\frac{-28\ \text{kcal/mol}}{RT}\right) \quad (15)$$

$$K_G(\text{low } T) = (1.2 \times 10^6\ \text{Torr}^{-1}) \exp\left(\frac{-14.7\ \text{kcal/mol}}{RT}\right) \quad (16)$$

$$K_G(\text{high } T) = (1.6 \times 10^{-8}\ \text{Torr}^{-1}) \exp\left(\frac{42.1\ \text{kcal/mol}}{RT}\right) \quad (17)$$

The best fit of the data yields two expressions for the adsorption equilibrium constant K_G. At low temperatures ($T \leq 625$ °C) the activation energy is positive, E_{AG}(low T) = 14.7 kcal/mol. Since a simple adsorption process usually has a small activation energy while a desorption process has a relatively large activation energy, the equilibrium constant for a simple adsorption step has a negative activation energy, $E_A = E_{ads} - E_{des} \simeq -E_{des}$.[44] Therefore, the positive activation energy for K_G at low temperatures indicates that dissociative adsorption governs the low-temperature growth. At high temperatures K_G has a negative activation energy, E_{AG}(high T) = 42.1 kcal/mol as expected for a nondissociative adsorption. The difference between the two activation energies, E_{AG}(low T) − E_{AG}(high T), gives the energy barrier for the dissociative desorption process. It is interesting to note that this value (56.8 kcal/mol) corresponds to the Me–Ga bond strength in Me_3Ga (56.7 kcal/mol).[42] This suggests an adsorption mechanism where dissociative adsorption of Me_3Ga dominates at low temperatures ($T \leq 625$ °C) while adsorption of MeGa formed in the gas phase is the major species arriving at the surface at temperatures above 625 °C. This picture is consistent with mass spectroscopy data showing

(44) Papapolymerou, G. A.; Schmidt, L. D. *Langmuir* **1985**, *1*, 488.

nearly complete pyrolysis of Me_3Ga to MeGa at temperatures above 600 °C and pressures similar to those used in this study.[18]

The above analysis of growth data for four different organometallic arsenic sources combined with either Me_3Ga or Et_3Ga shows that a model based on reversible adduct formation between arsenic and gallium source compounds and subsequent gas-phase reactions depleting film precursors in competition with the growth process is consistent with the experimental observations. However, adduct formation has not been reported in MOCVD growth of GaAs from t-$BuAs_2$ and Me_3Ga at atmospheric pressures.[3,4,8,14] Fundamental organometallic studies[30,32] as well as the recent emphasis on the use of adducts as source materials[23-28] demonstrate that donor–acceptor complexes form between arsenic and gallium compounds used in the present study. The question is whether the adduct is sufficiently stable to survive in the entrance zone and undergo internal rearrangement or whether it falls apart into the original alkyls. The microbalance reactor, used in the present study, has a relatively small heated volume in contrast to standard MOCVD systems, which also have long entrance zones. Furthermore, the microbalance system operates at low pressure, so that the growth is controlled by chemical kinetics, while mass-transfer influences the growth in atmospheric MOCVD reactors.[1] This difference is reflected in the large growth rates, ~ 20–30 μm/h, measured in the microbalance system in contrast to 1–5 μm/h achieved in conventional systems. The variation in growth rate with flow rates, which reveals the presence of adduct-related parasitic reactions in this work, is confined to growth rates higher than those typically measured in standard systems. Thus, it is possible that transport effects mask the adduct-related deposition phenomena in conventional reactors. Furthermore, because of the time-consuming task of obtaining growth rate data in standard systems, relatively few growth rate data[2,4,8] have been reported compared to the large number of data points generated with the microbalance reactor. Perhaps an extensive study of growth rate variations with flow rates, feed combinations, source compounds, and growth temperatures would reveal a mechanism similar to the model proposed here. Ultimately, the question about the actual growth mechanism will have to be resolved through careful spectroscopic identification of possible adduct intermediates and related decomposition reaction products.

Acknowledgment. This work was supported financially by the National Science Foundation (CBT-8351249, DMR 8704355) and Air Products and Chemicals. We are grateful to S. Brandon and M. Hoveland for help with the mass spectrometer and characterization studies. We also thank T. F. Kuech for help with photoluminescence and American Cyanamid for assistance with the t-$BuAsH_2$.

Registry No. GaAs, 1303-00-0; Et_3Ga, 1115-99-7; Me_3Ga, 1445-79-0; Me_3As, 617-75-4; Et_3As, 617-75-4; t-$BuAsH_2$, 4262-43-5; $PhAsH_2$, 822-65-1.

Surface Characterization of Radio Frequency Water Plasma Treated and Annealed Polycrystalline Tin Oxide Thin Films

Michael J. Tarlov† and John F. Evans*

Department of Chemistry, University of Minnesota, Minneapolis, Minnesota 55455

Received May 11, 1989

Angle-resolved X-ray photoelectron spectroscopy (AR-XPS) and electron energy loss spectroscopy (EELS) have been used to examine the consequences of the interaction of radio frequency water plasmas with polycrystalline tin oxide surfaces. Results from AR-XPS and EELS indicate that an extensive surface hydroxylation or "gel" layer (>10 Å) does not form on the tin oxide surface from exposure to atmosphere and/or water plasma treatment. Surface hydroxyl coverages determined by AR-XPS are a factor of 3 lower than those calculated from crystallographic models. Annealing of water plasma treated tin oxide films in ultrahigh vacuum results in the desorption of water, dehydroxylation of the surface, and creation of oxygen vacancies. AR-XPS data indicate a uniform concentration of oxygen vacancies over a sampling depth of approximately 15 Å. Water plasma treatment of oxygen-deficient tin oxide surfaces created by annealing in ultrahigh vacuum eliminates oxygen vacancies and restores Sn^{4+} valency in the surface region.

Introduction

Tin oxide (SnO_2) is an n-type, wide-bandgap (3.6 eV), metal oxide semiconductor.[1-3] When doped with antimony or fluorine, it becomes a quasimetallic conductor while retaining optical transparency in the visible region and a high reflectivity for infrared radiation. Many methods exist for the deposition of highly conductive, transparent, tin oxide films. This has allowed them to be used as transparent heating elements, heat refleting shields, and transparent electrical contacts.[4-6] In addition, tin oxide has been widely used as a gas-sensing element for the detection of H_2, CO, hydrocarbons, and alcohols.[7,8]

†Permanent Address: Chemical Process Metrology Division, National Institute of Standards and Technology, Gaithersburg, MD 20899.

(1) Jarzebski, Z. M.; Marton, J. P. *J. Electrochem. Soc.* **1976**, *123*, 199c.
(2) Jarzebski, Z. M.; Marton, J. P. *J. Electrochem. Soc.* **1976**, *123*, 299c.
(3) Jarzebski, Z. M.; Marton, J. P. *J. Electrochem. Soc.* **1976**, *123*, 333c.
(4) DeWaal, H.; Simonis, F. *Thin Solid Films* **1981**, *77*, 253.
(5) Frank, G.; Kauer, H.; Köstlin, L.; Kauer, E. *Thin Solid Films* **1981**, *77*, 107.
(6) Manifacier, J. C. *Thin Solid Films* **1982**, *100*, 297.
(7) McAleer, J. F.; Mosely, P. T.; Norris, J. O. W.; Williams, D. E. *J. Chem. Soc., Faraday Trans. 1* **1988**, *83*, 1323.
(8) McAleer, J. F.; Mosely, P. T.; Norris, J. O. W.; Williams, D. E.; Tofield, B. C. *J. Chem. Soc., Faraday Trans. 1* **1988**, *84*, 441.

0897-4756/90/2802-0049$02.50/0 © 1990 American Chemical Society